Letter

Attosecond photoionization delays in molecules: The role of nuclear motion

Adrián J. Suñer-Rubio,[1] Christoph Lemell,[2] Roger Y. Bello,[3] Joachim Burgdörfer,[2] Alicia Palacios,[1,4,5] and Fernando Martín[1,6]

[1]*Departamento de Química, Módulo 13, Universidad Autónoma de Madrid, 28049 Madrid, Spain*
[2]*Institute for Theoretical Physics, Vienna University of Technology, Wiedner Hauptstr. 8-10, A-1040 Vienna, Austria*
[3]*Departamento de Química Física Aplicada, Módulo 14, Universidad Autónoma de Madrid (UAM), 28049 Madrid, Spain*
[4]*Condensed Matter Physics Center (IFIMAC), Universidad Autónoma de Madrid (UAM), 28049 Madrid, Spain*
[5]*Institute of Advanced Research in Chemical Sciences (IAdChem), Universidad Autónoma de Madrid (UAM), 28049 Madrid, Spain*
[6]*Instituto Madrileño de Estudios Avanzados IMDEA Nanociencia, Cantoblanco, 28049 Madrid, Spain*

(Received 25 January 2024; accepted 22 April 2024; published 20 June 2024)

Molecular photoionization delays are often analyzed by assuming that nuclei remain fixed during the ionization process since they move much more slowly than electrons. However, recent high-energy resolution and multicoincidence experiments have shown that nuclear motion can have a significant and visible effect on the measured ionization delays on the attosecond time scale. To analyze this behavior, we have chosen the simplest of all molecules, H_2^+, and performed nearly exact calculations of streaking and RABBIT (reconstruction of attosecond beatings by interferences in two-photon transitions) spectra by solving the time-dependent Schrödinger equation in full dimensionality, and retrieved the corresponding photoionization delays. We show that, when two-center effects are at play, nuclear motion is responsible for a substantial increase of the photoionization delays, in particular of the so-called continuum-continuum delays. The magnitude of such an increase is comparable to the absolute values of the measured delays.

DOI: 10.1103/PhysRevResearch.6.L022066

Following the first realization of attosecond pulses [1,2], photoionization time delays have been extensively investigated in atoms ([3–7] and References therein) and, more recently, in molecular targets [8–16]. One of the key issues has been to relate the single-photon ionization delays, or Eisenbud-Wigner-Smith (EWS) delays [17–19], to the delays extracted either from attosecond electron streaking [20–22] or two-photon interferometric measurements [2,23], both of which combine the XUV pulses needed to ionize the system with IR fields. Although the problem has now been satisfactorily solved in atomic systems [3,4,6,24–28], this is not the case for molecules due to the presence of the additional nuclear degrees of freedom, which complicates the analysis and thus calls for extension of the concepts developed for atoms. Up to now, interpretation of measured delays is mostly based on the assumption that nuclei do not move (fixed-nuclei approximation, FNA), using the fact that, for not-too-low kinetic energy of the ejected electron, nuclei move much more slowly than electrons.

Recent experimental work on H_2 [14,29], N_2 [8,15,30], and CH_4 [31] has shown, however, that photoionization delays may depend not only on the kinetic energy of the emitted electron but also on the energy deposited in the vibrational and dissociative degrees of freedom of the remaining cation, i.e., on the sharing of the excess photon energy between electrons and nuclei. Furthermore, photoionization delays are expected to be sensitive to molecular orientation and the multicenter character of the molecular potential [32]. To establish a solid theoretical framework for molecular photoionization time delays and to gauge the applicability of extraction protocols for atoms and molecules, one should ideally solve the time-dependent Schrödinger equation in full dimensionality by including all electronic and nuclear degrees of freedom. In this work, we have accomplished this goal by applying the nearly exact spectral method described in Refs. [33–35] to evaluate attosecond electron streaking and reconstruction of attosecond beatings by interference of two-photon transitions (RABBIT) spectra for the simplest and most fundamental molecule, the H_2^+ molecular ion.

We show that, for specific molecular orientations with respect to the light polarization direction, calculated photoionization delays retrieved from either streaking or RABBIT spectra are significantly larger when the nuclear dynamics is fully accounted for as compared to the limit of fixed nuclei. Surprisingly, the influence of the nuclear degree of freedom is more pronounced for the time delay related to the IR-induced continuum-continuum coupling than the time delay of the XUV-induced bound-free transition is perturbed. This enhancement of the time delay is found to be nearly identical for attosecond streaking employing single-attosecond pulses (SAP) and for RABBIT involving attosecond pulse trains (APT). We attribute this behavior to the interplay between enhanced two-center effects in the presence of the IR field and the spreading of the molecular wave packet. The important

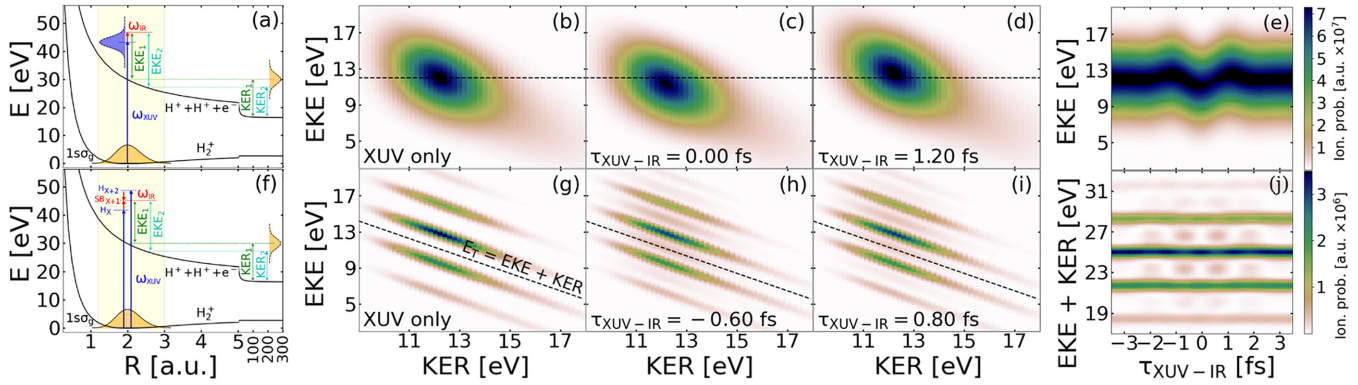

FIG. 1. Simulation of photoionization of the H_2^+ molecule in a streaking (upper row) and RABBIT (lower row) scenario. Panels (a) and (f) show the potential energy curves of the ground state of H_2^+ ($1s\sigma_g$) and the ionization threshold ($1/R$), where R is the internuclear distance, and the vertical transition after absorption of a single XUV photon (blue arrow). Also shown is the absorption or emission of a single IR photon (red arrows) in a continuum-continuum transition. The expected EKEs and KERs are also indicated (green and cyan lines and labels). (b) and (g): photoionization coincidence maps after absorption of the XUV radiation (no IR included). (c)–(d) and (h)–(i): corresponding photoionization coincidence maps in the presence of the IR field for two different time delays between the XUV and IR pulses. The black dashed horizontal lines in (c) and (d) indicate the EKE at which the largest ionization probability is obtained with XUV pulses only. The black dashed diagonal line in (h) and (i) represents a typical energy conservation line, EKE + KER, resulting from the sharing of the excess photon energy between the electron and the nuclei. (e): streaking spectrogram (photoelectron spectrum as a function of the XUV-IR delay) at a fixed KER of 12.2 eV. (j): RABBIT spectrogram (photoelectron spectrum as a function of the XUV-IR delay) as the fixed total energy indicated by a cut perpendicular to the black diagonal line in panels (h) and (i).

implication of the present result is that physically meaningful measurements of photoionization delays in molecules require determining both photoelectron and nuclear kinetic energies, and, ideally, molecular orientation. An illustration of the streaking and RABBIT protocols for H_2^+ is given in Fig. 1. In streaking [Fig. 1(a)], an XUV single attosecond pulse ionizes the molecule, leading to an electron kinetic energy (EKE) distribution that roughly follows the envelope of the XUV pulse in the frequency domain. The IR pulse streaks the electron in the continuum, thus shifting this distribution in energy. In RABBIT [Fig. 1(f)], an XUV attosecond pulse train gives rise to harmonic peaks in the photoelectron spectrum [H_X and H_{X+2} in Fig. 1(f)]. The IR induces transitions to states between two consecutive harmonics, generating sidebands [SB_{X+1} in Fig. 1(f)]. In both protocols, ionization leaves two bare protons behind, leading to Coulomb explosion in which the nuclei acquire kinetic energy (kinetic energy release, KER). The range of accessible KERs is roughly determined by the width of the Franck-Condon region (yellow vertical band). In the streaking calculations, we have used a SAP with 40 eV central frequency, 1 fs total duration ($\cos^2$ envelope, FWHM = 364 as), 3×10^{10} W/cm^2 peak intensity and cosine-square envelope, and an IR pulse with 1.65 eV central frequency, 6 fs duration, 10^{11} W/cm^2 peak intensity and cosine-square envelope. In the RABBIT calculations, we have employed an APT with 7 identical XUV pulses with the same central frequency and peak intensity as in the streaking calculations, with 800 as duration each and separated by 1.25 fs, with a global Gaussian envelope; the IR pulse is also the same as before except for a slightly larger duration of 8 fs. The range of photon energies covered by the chosen pulses is representative of current streaking and RABBIT experiments.

Figure 1 also shows the calculated photoionization coincidence maps, in EKE and KER, for ionization by a SAP [Fig. 1(b)] and an APT XUV pulse [Fig. 1(g)] of an H_2^+ molecule parallel to the polarization direction and the electron ejected in this same direction ($\theta_e = 0°, \phi_e = 0°$, and $\theta_N = 0°, \phi_N = 0°$) in the absence of an IR probing pulse. Figs. 1(c)–1(d) and 1(h)–1(i) display the corresponding streaking or RABBIT coincidence maps for two different time delays between the XUV and IR pulses. In the streaking scenario, the probability distribution in electronic kinetic energy oscillates as a function of XUV-IR delay shown for two typical delays [Figs. 1(c)–1(d)]. In the RABBIT coincidence maps, both harmonic and side bands follow total energy conservation lines E_T = EKE + KER, reflecting the fact that the excess photon energy is shared between electrons and nuclei [Figs. 1(h)–1(i)]. Figure 1(e) displays a typical streaking spectrogram as a function of the XUV-IR delay, Fig. 1(j) the corresponding RABBIT spectrum for a cut perpendicular to the direction of energy conservation exhibiting the typical oscillations in the sidebands as a function of the XUV-IR delay. An important point to stress is that photoionization amplitudes, hence any property that can be extracted from them, including photoionization delays, depend significantly on both EKE and KER. In other words, streaking and RABBIT spectra depend on the state in which the remaining ionic species is left. The same applies to the EWS delays. Indeed, the asymptotic phases of the wave function as well as the partial derivatives of these phases with respect to electron energy (the EWS delays) depend on both electron (EKE) and nuclear (KER) energies, as shown by the EKE-KER two-dimensional plots in Fig. 2(a).

Photoionization time delays have been retrieved from streaking spectra by fitting to

$$\mathbf{p_f}(\tau) = \mathbf{p_0} - \alpha \mathbf{A}_{\mathrm{IR}}(\tau + \tau_S), \tag{1}$$

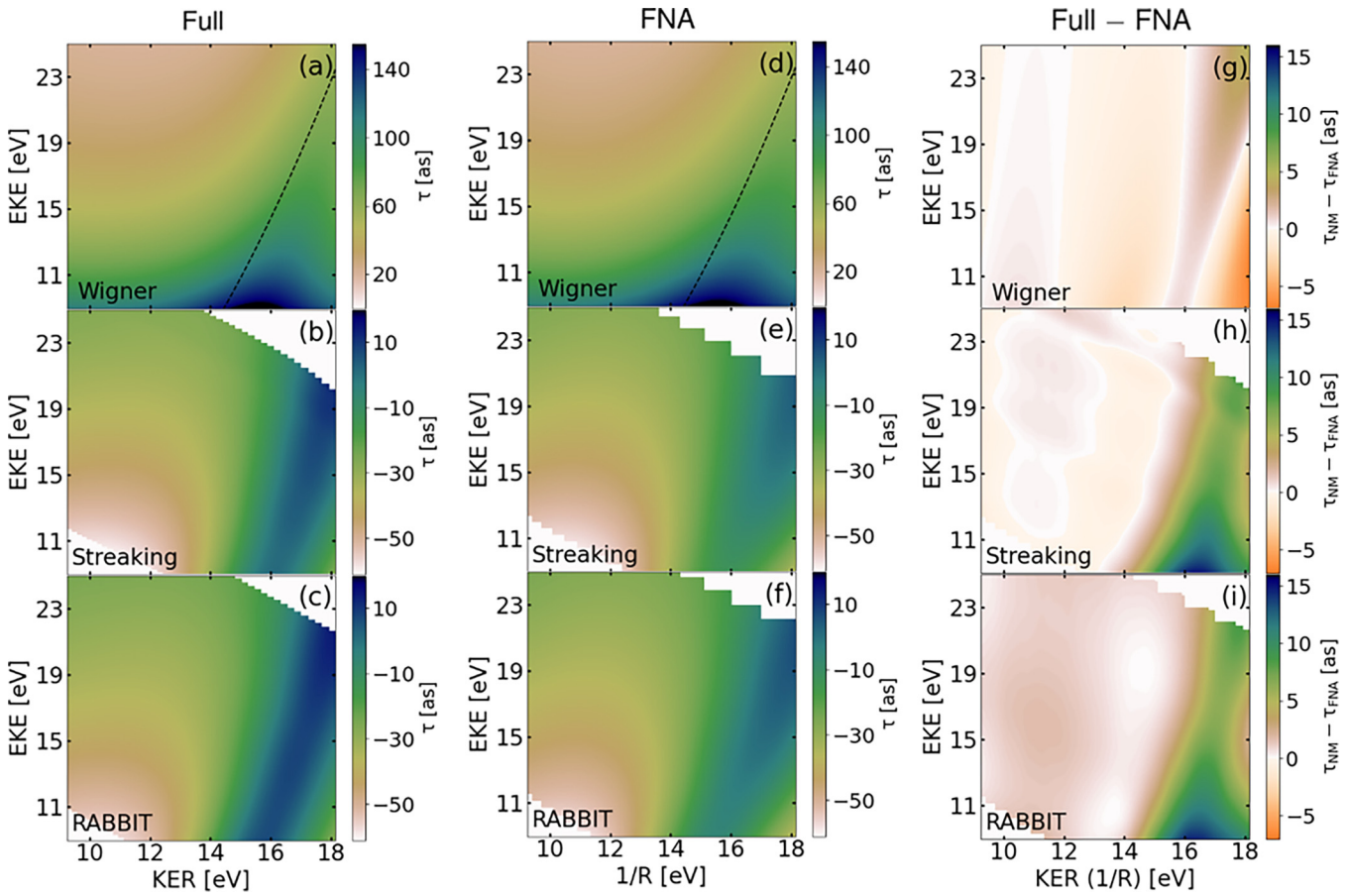

FIG. 2. Photoionization time delays resulting from the full calculation (left column) and the FNA (central column) for H_2^+ molecules parallel to the polarization direction and electron ejection along this same direction. The right column shows the difference between the former two. (a),(d),(g): photoionization EWS delay $\tau_{\rm EWS}^{bc}$, (b),(e),(h): streaking delay τ_s, (c),(f),(i): RABBIT delay τ_R. The dashed lines in (a) and (d) show the confinement line $\mathrm{EKE}(R) = \pi^2/(2R^2) - 2/R$ (see text).

where τ is the delay between the XUV and IR pulses, $\mathbf{p_0}$ is the asymptotic momentum of the photoelectron in the absence of the streaking IR field for a given KER, τ_S is the observed streaking time delay, and α ($\simeq 1$) is a fitting parameter introduced to match the values of the vector potential $\mathbf{A}_{\rm IR}$ to those of the final momentum of the electron $\mathbf{p_f}$ at the chosen KER. Since the final linear momentum of the electron is given by a probability distribution, due to the bandwidth of the XUV and IR pulses [see Figs. 1(a) and 1(e)], we apply Eq. (1) to the mean value of the final momentum. In the case of RABBIT, photoionization delays have been obtained by fitting the photoionization probability for a given (KER, EKE) and for each sideband S_R to

$$S_R = \alpha + \beta \cos[2\omega(\tau - \tau_R)], \tag{2}$$

where τ is the delay between the XUV and IR pulses, ω is the central frequency of the IR pulse (no redshift included), τ_R is the RABBIT time delay, and α and β are two fitting parameters.

The full dimensional simulations of the EWS time delay $\tau_{\rm EWS}^{bc}$ [Fig. 2(a)], of the streaking delay τ_s [Fig. 2(b)], as well as of the RABBIT delay τ_R [Fig. 2(c)], all of which include the nuclear Coulomb explosion dynamics, significantly differ from the corresponding results in fixed-nuclei approximation [Figs. 2(d)–2(f)]. The differences between the time delays obtained from these two approaches are shown in Figs. 2(g)–2(i). For a direct comparison with results of the full calculations, the results in FNA are plotted as a function of EKE and $1/R$, since KER $\simeq 1/R$ according to the widely used reflection approximation (see, e.g., Refs. [36,37]). These delays have been obtained for molecules parallel to the polarization direction and electrons ejected along this same direction. Results for the perpendicular orientation are given in the Supplemental Materials (SM) [38].

While the differences between the results of the full calculation and the FNA for $\tau_{\rm EWS}^{bc}$ are rather small [Fig. 2(g)], the differences for the streaking or RABBIT delays are significant and can reach values up to ∼15 as, i.e., comparable in magnitude to the values τ_s and τ_R themselves. The point to be stressed is that the streaking and RABBIT delays closely agree with each other ($\tau_s \approx \tau_R$) for all EKE and KER. Therefore, the observed differences full − FNA [Figs. 2(h)–2(i)] can be identified as an unambiguous signature of a strong influence of the nuclear motion on the continuum-continuum coupling subsequent to the primary ionization event.

The fact that for perpendicular emission (see Fig. 2 in SM) a similarly strong and energy-dependent deviation is absent, provides an important clue as to its origin. Within the range of EKE accessible by the spectral distribution of the present XUV pulses, electronic two-center destructive interference

effects are only expected for parallel emission when the wavelength of the ejected electron is comparable to the distance R between the two protons, i.e., its momentum p satisfies $pR \simeq (2n+1)\pi$ (the so-called confinement effect, see Ref. [39]). Within the FNA, these interferences have been previously shown [11] to drastically modify the time delays where, in general, both large delays ($\tau > 0$) and advances ($\tau < 0$) are possible. The present results suggest that two-center effects are not only important to describe ionization by the XUV pulses, but they can play an even more important role in the way the electron is streaked by the IR field or absorbs/emits IR photons. The additional delay due to electron confinement shows up in the region near the confinement line approximately given by $\mathrm{EKE}(R) = p^2(R)/2 + V_{\mathrm{pot}}(R) = (2n+1)^2\pi^2/(2R^2) - 2/R$ [see Figs. 2(a), 2(d) for $n = 0$ and Fig. 1 in SM for $n \geqslant 0$], where the first term represents the mean molecular kinetic energy of the confined electron and the second one the mean potential energy felt by the electron. The width in KER of the confinement region mainly reflects the initial spread of the nuclear wave packet at the instant of photoionization. In the absence of the IR field, the additional delay due to nuclear motion is at most $\pm 3-6$ as [Fig. 2(g)]. This additional delay is due to the fact that the interaction with the XUV pulse coherently ionizes the molecule from its distribution of nuclear distances R, which obviously cannot be described within the FNA.

To analyze why nuclear motion leads to a more pronounced increase of the confinement time in the presence of the IR, let us consider a typical point in the EKE-KER plane in the confinement region, EKE ~ 12 eV and KER ~ 16 eV ($R \sim 1.7$ a.u. in the FNA). According to Fig. 2(a), the EWS photoionization time delay in the presence of the two-center effect is about 130 as and, thus, enhanced by confinement by about 65 as relative to that of the same EKE-KER point in the absence of confinement [perpendicular polarization direction, see Fig. 2(a) in SM]. This increase in EWS delay is comparable to the time a classical electron needs for a round trip between the nuclei, $\Delta t = 2R/p = 2R^2/\pi$. In turn, this additional time delay modifies the coupling of the electron to the IR field in the presence of the spreading nuclear wave packet. In the absence of confinement, the increase in streaking (or RABBIT) time delay due to the spreading wave packet at this EKE-KER point is about 6 as [Figs. 2(h), 2(i) in SM]. Scaling this by the confinement-enhanced time delay $\tau^{\parallel}_{\mathrm{EWS}}/\tau^{\perp}_{\mathrm{EWS}} \approx 2$ gives ~ 12 as in good agreement with the values shown in Figs. 2(h) and 2(i) in the chosen EKE-KER region. We thus conclude that it is the interplay between nuclear motion and the confinement-enhanced electron-IR field coupling that leads to the remarkable change in RABBIT (or streaking) time delays for molecular photoionization. To further explore the quantum nature of this effect we have performed classical trajectory Monte Carlo (CTMC) calculations, in which both the electron and the nuclei are treated classically [25]. Over-barrier quantum reflections which provide the underpinning to the temporal confinement of the electron in between the two nuclei [39] are absent in the classical electron dynamics. In Fig. 3 we compare the photoionization time delays as a function of the EKE resulting from full classical and quantum calculations both accounting for the nuclear degree of freedom for two prototypical cases. Figure 3(a) shows the delays for parallel emission, where two-center interferences prominently appear in the present spectral range of the XUV pulse and for a relatively high KER $\simeq 17$ eV. By contrast, Fig. 3(b) presents corresponding results for perpendicular emission, where two-center effects are absent at these photon energies. While the CTMC agrees well with the full quantum simulation for perpendicular emission down to surprisingly low EKE ($\simeq 10$ eV), it fails by up to $\sim$100 as when two-center effects are important.

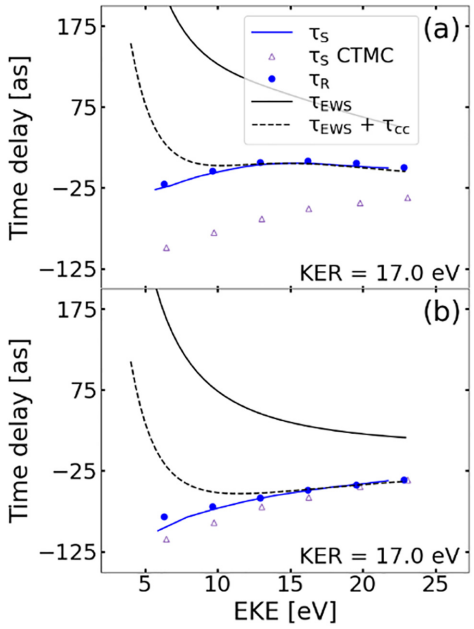

FIG. 3. Photoionization time delays for the H_2^+ molecule for (a) emission parallel to the internuclear axis and (b) perpendicular to it at a KER of 17 eV. Black solid lines: EWS time delays. Blue solid lines: streaking delays. Blue dots: RABBIT delays. Purple triangles: streaking delays predicted by a fully classical CTMC simulation in which two-center interferences are absent. Black dashed lines: RABBIT (or streaking) delays predicted by the sum $\tau^{bc}_{\mathrm{EWS}} + \tau_{\mathrm{CC}}$ [41] (or $\tau^{bc}_{\mathrm{EWS}} + \tau_{\mathrm{CLC}}$ [42]) with τ_{CC} (τ_{CLC}) for an atomic Coulomb field.

Figure 3 also shows the prediction of the additivity rule $\tau_R = \tau^{bc}_{\mathrm{EWS}} + \tau_{\mathrm{CC}}$ or, equivalently, $\tau_s = \tau^{bc}_{\mathrm{EWS}} + \tau_{\mathrm{CLC}}$ well established for atoms [40–42]. Both τ_{CC} and τ_{CLC} account for the coupling between the electron in the continuum and the IR field in the vicinity of the ionic core. When applied to the H_2^+ molecule, the additivity rule still holds as long as EKE $\gtrsim$ KER but dramatically fails when the Coulomb-explosion energy KER dominates over the electronic kinetic energy EKE. This finding underscores the important influence of the nuclear motion on the coupling of the outgoing electron and IR field and suggests a potential modification of the CLC (or CC) contribution to the time delay for molecules when multicenter and confinement effects become important.

In conclusion, we have shown that nuclear motion has a strong influence on photoionization time delays retrieved from streaking and RABBIT spectra when multicenter effects are at play. Surprisingly, this influence is most prominently

observed in the coupling between the IR field and the continuum electron even though direct coupling to nuclear motion is negligible. The EWS time delay associated with the transition from the bound state to the molecular ionization continuum, on the other hand, can be reasonably well approximated by the fixed nuclei approximation. The molecular correction to the IR induced delays, τ_{CLC} or τ_{CC}, is largest in the spectral region where two-center interference or confinement effects significantly contribute and where the magnitude of the KER in the dissociation process becomes comparable to the asymptotic energy of the emitted electron. At higher energies and outside the region of two-center interferences one can safely rely on the fixed nuclei approximation in combination with the reflection approximation to interpret the observed delays as empirically demonstrated for N_2 [15] and CF_4 [32].

Similar effects on photoionization delays as those reported here for H_2^+ are expected to appear for other molecules and molecular ions when dissociation channels accompanied by Coulomb explosion and emission of protons are accessible. We also note that, in most experiments, delays are measured relative to a reference measurement in order to subtract contributions from an uncompensated attochirp of the XUV pulses. As such a reference signal from an atom is free of any two-center effects, the experimentally accessible delay differences should allow unravelling confinement-induced time delays undistorted by an attochirp.

Work funded by the Ministerio de Ciencia, Innovación y Universidades (Spain) through Grants No. PID2022-138288NB-C31 and No. PID2022-138288NB-C32, the Severo Ochoa Programme for Centres of Excellence in R & D (Grant No. CEX2020-001039-S) and the María de Maeztu Programme for Units of Excellence in R&D (Grant No. CEX2018-000805-M), and developed in the framework of the COST action Grant No. CA18222. Attosecond Chemistry (AttoChem) supported by European Cooperation in Science and Technology, the Austrian Science Funds (FWF) Grant No. P35539-N and the International Max Planck Research School Advanced Photon Science (IMPRS-APS). A.J.S.-R. acknowledges MICINN for the Formación del Profesorado Universitario Grant No. FPU19/01707 and the Residencia de Estudiantes for a scholarship for graduate students. All calculations were performed at the Marenostrum Barcelona Supercomputer Center of the Red Española de Supercomputación and the Centro de Computación Científica of Universidad Autónoma de Madrid.

[1] M. Henschel, R. Kienberger, C. Spielmann, G. A. Reider, N. Milosevic, T. Brabec, P. Corkum, U. Heinzmann, M. Drescher, and F. Krausz, Attosecond metrology, Nature (London) **414**, 509 (2001).

[2] P. M. Paul, E. S. Toma, P. Breger, G. Mullot, F. Augé, P. Balcou, H. G. Muller, and P. Agostini, Observation of a train of attosecond pulses from high harmonic generation, Science **292**, 1689 (2001).

[3] M. Schultze, M. Fieß, N. Karpowicz, J. Gagnon, M. Korbman, M. Hofstetter, S. Neppl, A. L. Cavalieri, Y. Komninos, T. Mercouris, C. A. Nicolaides, R. Pazourek, S. Nagele, J. Feist, J. Burgdörfer, A. M. Azzeer, R. Ernstorfer, R. Kienberger, U. Kleineberg, E. Goulielmakis *et al.*, Delay in photoemission, Science **328**, 1658 (2010).

[4] D. Guénot, D. Kroon, E. Balogh, E. W. Larsen, M. Kotur, M. Miranda, T. Fordell, P. Johnsson, J. Mauritsson, M. Gisselbrecht, K. Varj, C. L. Arnold, T. Carette, A. S. Kheifets, E. Lindroth, A. LHuillier, and J. M. Dahlström, Measurements of relative photoemission time delays in noble gas atoms, J. Phys. B **47**, 245602 (2014).

[5] L. Cattaneo, J. Vos, M. Lucchini, L. Gallmann, C. Cirelli, and U. Keller, Comparison of attosecond streaking and RABBITT, Opt. Express **24**, 29060 (2016).

[6] M. Isinger, R. J. Squibb, D. Busto, S. Zhong, A. Harth, D. Kroon, S. Nandi, C. L. Arnold, M. Miranda, J. M. Dahlström, E. Lindroth, R. Feifel, M. Gisselbrecht, and A. LHuillier, Photoionization in the time and frequency domain, Science **358**, 893 (2017).

[7] J. Söngård, J. M. Dahlström, and E. Lindroth, Study of the possibilities with combinations of circularly and linearly polarized light for attosecond delay investigations, J. Phys. B: At. Mol. Opt. Phys. **53**, 134003 (2020).

[8] S. Haessler, B. Fabre, J. Higuet, J. Caillat, T. Ruchon, P. Breger, B. Carre, E. Constant, A. Maquet, E. Mevel, P. Salieres, R. Taïeb, and Y. Mairesse, Phase-resolved attosecond near-threshold photoionization of molecular nitrogen, Phys. Rev. A **80**, 011404(R) (2009).

[9] G. Sansone, F. Kelkensberg, J. Perez-Torres, F. Morales, M. Kling, W. Siu, O. Ghafur, P. Johnsson, M. Swoboda, E. Benedetti, F. Ferrari, F. Ipine, J. Sanz-Vicario, S. Zherebtsov, I. Znakovskaya, A. L'Huillier, M. Ivanov, M. Nisoli, F. Martín, and M. Vrakking, Electron localization following attosecond molecular photoionization, Nature (London) **465**, 763 (2010).

[10] F. Calegari, D. Ayuso, A. Trabattoni, L. Belshaw, S. De Camillis, S. Anumula, F. Frassetto, L. Poletto, A. Palacios, P. Decleva, J. B. Greenwood, F. Martín, and M. Nisoli, Ultrafast electron dynamics in phenylalanine initiated by attosecond pulses, Science **346**, 336 (2014).

[11] Q.-C. Ning, L.-Y. Peng, S.-N. Song, W.-C. Jiang, S. Nagele, R. Pazourek, J. Burgdörfer, and Q. Gong, Attosecond streaking of Cohen-Fano interferences in the photoionization of H_2^+, Phys. Rev. A **90**, 013423 (2014).

[12] M. Huppert, I. Jordan, D. Baykusheva, A. von Conta, and H. J. Wörner, Attosecond delays in molecular photoionization, Phys. Rev. Lett. **117**, 093001 (2016).

[13] D. Baykusheva and H. J. Wörner, Theory of attosecond delays in molecular photoionization, J. Chem. Phys. **146**, 124306 (2017).

[14] L. Cattaneo, J. Vos, R. Bello, A. Palacios, S. Heuser, L. Pedrelli, M. Lucchini, C. Cirelli, F. Martín, and U. Keller, Attosecond coupled electron and nuclear dynamics in dissociative ionization of H_2, Nat. Phys. **14**, 733 (2018).

[15] S. Nandi, E. Plésiat, S. Zhong, A. Palacios, D. Busto, M. Isinger, L. Neoričić, C. L. Arnold, R. J. Squibb, R. Feifel, P. Decleva, A. L'Huillier, F. Martín, and M. Gisselbrecht, Attosecond timing of electron emission from a molecular shape resonance, Sci. Adv. **6**, eaba7762 (2020).

[16] S. Patchkovskii, J. Benda, D. Ertel, and D. Busto, Theory of nuclear motion in RABBITT spectra, Phys. Rev. A **107**, 043105 (2023).
[17] L. Eisenbud, The formal properties of nuclear collisions, Ph.D. thesis, Princeton University, 1948.
[18] E. P. Wigner, Lower limit for the energy derivative of the scattering phase shift, Phys. Rev. **98**, 145 (1955).
[19] F. T. Smith, Lifetime matrix in collision theory, Phys. Rev. **118**, 349 (1960).
[20] E. Constant, V. D. Taranukhin, A. Stolow, and P. B. Corkum, Methods for the measurement of the duration of high-harmonic pulses, Phys. Rev. A **56**, 3870 (1997).
[21] J. Itatani, F. Quere, G. L. Yudin, M. Y. Ivanov, F. Krausz, and P. B. Corkum, Attosecond streak camera, Phys. Rev. Lett. **88**, 173903 (2002).
[22] E. Goulielmakis, M. Uiberacker, R. Kienberger, A. Baltuska, V. Yakovlev, A. Scrinzi, T. Westerwalbesloh, U. Kleineberg, U. Heinzmann, M. Drescher, and F. Krausz, Direct measurement of light waves, Science **305**, 1267 (2004).
[23] H. Muller, Reconstruction of attosecond harmonic beating by interference of two-photon transitions, Appl. Phys. B **74**, s17 (2002).
[24] K. Klünder, J. M. Dahlström, M. Gisselbrecht, T. Fordell, M. Swoboda, D. Guénot, P. Johnsson, J. Caillat, J. Mauritsson, A. Maquet, R. Taïeb, and A. L'Huillier, Probing single-photon ionization on the attosecond time scale, Phys. Rev. Lett. **106**, 143002 (2011).
[25] S. Nagele, R. Pazourek, J. Feist, K. Doblhoff-Dier, C. Lemell, K. Tökesi, and J. Burgdörfer, Time-resolved photoemission by attosecond streaking: extraction of time information, J. Phys. B **44**, 081001 (2011).
[26] S. Zhong, J. Vinbladh, D. Busto, R. J. Squibb, M. Isinger, L. Neoričić, H. Laurell, R. Weissenbilder, C. L. Arnold, R. Feifel, J. M. Dahlström, G. Wendin, M. Gisselbrecht, E. Lindroth, and A. L'Huillier, Attosecond electron–spin dynamics in Xe 4d photoionization, Nat. Commun. **11**, 5042 (2020).
[27] C. Alexandridi, D. Platzer, L. Barreau, D. Busto, S. Zhong, M. Turconi, L. Neoričić, H. Laurell, C. L. Arnold, A. Borot, J.-F. Hergott, O. Tcherbakoff, M. Lejman, M. Gisselbrecht, E. Lindroth, A. L'Huillier, J. M. Dahlström, and P. Salieres, Attosecond photoionization dynamics in the vicinity of the Cooper minima in argon, Phys. Rev. Res. **3**, L012012 (2021).
[28] J. Peschel, D. Busto, M. Plach, M. Bertolino, M. Hoflund, S. Maclot, J. Vinbladh, H. Wikmark, F. Zapata, E. Lindroth, M. Gisselbrecht, J. M. Dahlström, A. L'Huillier, and P. Eng-Johnsson, Attosecond dynamics of multi-channel single photon ionization, Nat. Commun. **13**, 5205 (2022).
[29] L. Cattaneo, L. Pedrelli, R. Y. Bello, A. Palacios, P. D. Keathley, F. Martín, and U. Keller, Isolating attosecond electron dynamics in molecules where nuclei move fast, Phys. Rev. Lett. **128**, 063001 (2022).
[30] V. J. Borràs, J. Gonzalez-Vazquez, L. Argenti, and F. Martín, Attosecond photoionization delays in the vicinity of molecular Feshbach resonances, Sci. Adv. **9**, eade3855 (2023).
[31] X. Gong, E. Plésiat, A. Palacios, S. Heck, F. Martín, and H. J. Wörner, Attosecond delays between dissociative and non-dissociative ionization of polyatomic molecules, Nat. Commun. **14**, 4402 (2023).
[32] H. Ahmadi, E. Plésiat, M. Moioli, F. Frassetto, L. Poletto, P. Decleva, C. D. Schröter, T. Pfeiffer, R. Moshammer, A. Palacios, F. Martín, and G. Sansone, Attosecond photoionisation time delays reveal the anisotropy of the molecular potential in the recoil frame, Nat. Commun. **13**, 1242 (2022).
[33] A. Palacios, H. Bachau, and F. Martín, Enhancement and control of H_2 dissociative ionization by femtosecond VUV laser pulses, Phys. Rev. Lett. **96**, 143001 (2006).
[34] J. L. Sanz-Vicario, H. Bachau, and F. Martín, Time-dependent theoretical description of molecular autoionization produced by femtosecond xuv laser pulses, Phys. Rev. A **73**, 033410 (2006).
[35] A. Palacios, J. L. Sanz-Vicario, and F. Martín, Theoretical methods for attosecond electron and nuclear dynamics: applications to the H_2 molecule, J. Phys. B: At. Mol. Opt. Phys. **48**, 242001 (2015).
[36] H. D. Hagstrum, Ionization by electron impact in CO, N_2, NO, and O_2, Rev. Mod. Phys. **23**, 185 (1951).
[37] D. A. Horner, W. Vanroose, T. N. Rescigno, F. Martín, and C. W. McCurdy, Role of nuclear motion in double ionization of molecular hydrogen by a single photon, Phys. Rev. Lett. **98**, 073001 (2007).
[38] See Supplemental Material at http://link.aps.org/supplemental/10.1103/PhysRevResearch.6.L022066 for results of calculations with higher EKE or molecules oriented perpendicular to the polarization direction.
[39] J. Fernández, O. Fojón, A. Palacios, and F. Martín, Interferences from fast electron emission in molecular photoionization, Phys. Rev. Lett. **98**, 043005 (2007).
[40] R. Pazourek, S. Nagele, and J. Burgdörfer, Attosecond chronoscopy of photoemission, Rev. Mod. Phys. **87**, 765 (2015).
[41] J. Dahlström, D. Guénot, K. Klünder, M. Gisselbrecht, J. Mauritsson, A. LHuillier, A. Maquet, and R. Taïeb, Theory of attosecond delays in laser-assisted photoionization, Chem. Phys. **414**, 53 (2013).
[42] R. Pazourek, S. Nagele, and J. Burgdörfer, Time-resolved photoemission on the attosecond scale: opportunities and challenges, Faraday Discuss. **163**, 353 (2013).